Stochastic approach to Fisher and Kolmogorov, Petrovskii, and Piskunov wave fronts for species with different diffusivities in dilute and concentrated solutions

Gabriel Morgado[1,2], Bogdan Nowakowski[1], and Annie Lemarchand*[2]

[1]Institute of Physical Chemistry, Polish Academy of Sciences, Kasprzaka 44/52, 01-224 Warsaw, Poland

[2]Laboratoire de Physique Théorique de la Matière Condensée, Sorbonne Université, CNRS UMR 7600, 4 place Jussieu, case courrier 121, 75252 Paris CEDEX 05, France

July 22, 2020

* Corresponding author: Annie Lemarchand, E-mail: annie.lemarchand@sorbonne-universite.fr

Abstract

A wave front of Fisher and Kolmogorov, Petrovskii, and Piskunov type involving two species A and B with different diffusion coefficients D_A and D_B is studied using a master equation approach in dilute and concentrated solutions. Species A and B are supposed to be engaged in the autocatalytic reaction A+B $\rightarrow$ 2A. Contrary to the results of a deterministic description, the front speed deduced from the master equation in the dilute case sensitively depends on the diffusion coefficient of species B. A linear analysis of the deterministic equations with a cutoff in the reactive term cannot explain the decrease of the front speed observed for $D_B > D_A$. In the case of a concentrated solution, the transition rates associated with cross-diffusion are derived from the corresponding diffusion fluxes. The properties of the wave front obtained in the dilute case remain valid but are mitigated by cross-diffusion which reduces the impact of different diffusion coefficients.

1 Introduction

Wave fronts propagating into an unstable state according to the model of Fisher and Kolmogorov, Petrovskii, and Piskunov (FKPP) [1, 2] are encountered in many fields [3], in particular biology [4] and ecology [5]. Phenotype selection through the propagation of the fittest trait [6] and cultural transmission in neolithic transitions [7] are a few examples of applications of FKPP fronts. The model introduces a partial differential equation with a logistic growth term and a diffusion term.

The effect of non standard diffusion on the speed of FKPP front is currently investigated [8, 9, 10, 11] and we recently considered the propagation of a wave front in a concentrated solution in which cross-diffusion cannot be neglected [12]. Experimental evidence of cross-diffusion has been given in systems involving ions, micelles, surface, or polymer reactions and its implication in hydrodynamic instabilities has been demonstrated [13, 14, 15, 16, 17, 18]. In parallel, cross-diffusion is becoming an active field of research in applied mathematics [19, 20, 21, 22, 23, 24].

The sensitivity of FKPP fronts to fluctuations has been first numerically observed [25, 26]. An interpretation has been then proposed in the framework of a deterministic approach introducing a cutoff in the logistic term [27]. In mesoscopic or microscopic descriptions of the invasion front of A particles engaged in the reaction A + B → 2A, the discontinuity induced by the rightmost particle in the leading edge of species A profile amounts to a cutoff in the reactive term. The inverse of the number of particles in the reactive interface gives an estimate of the cutoff [28]. The study of the effect of fluctuations on FKPP fronts remains topical [29, 30]. In this paper we perform a stochastic analysis of a reaction-diffusion front of FKPP type in the case of two species A and B with different diffusion coefficients [31], giving rise to cross-diffusion phenomena in concentrated solutions.

The paper is organized as follows. Section 2 is devoted to a dilute system without cross-diffusion. The effects of the discrete number of particles on the front speed, the shift between the profiles of the two species and the width of species A profile are deduced from

a master equation approach. In section 3, we derive the expression of the master equation associated with a concentrated system inducing cross-diffusion and compare the properties of the FKPP wave front in the dilute and the concentrated cases. Conclusions are given in section 4.

2　Dilute system

We consider two chemical species A and B engaged in the reaction

$$\text{A} + \text{B} \xrightarrow{k} 2\,\text{A},\tag{1}$$

where k is the rate constant. The diffusion coefficient, D_A, of species A may differ from the diffusion coefficient, D_B, of species B.

In a deterministic approach, the reaction-diffusion equations are

$$\partial_t A = D_A \partial_x^2 A + kAB \tag{2}$$

$$\partial_t B = D_B \partial_x^2 B - kAB \tag{3}$$

where the concentrations of species A and B are denoted by A and B. The system admits wave front solutions propagating without deformation at constant speed. For sufficiently steep initial conditions and in particular step functions ($A(x, t = 0) = C_0 H(-x)$ and $B(x, t = 0) = C_0 H(x)$), where C_0 is constant and $H(x)$ is the Heaviside function, the minimum velocity

$$v^* = 2\sqrt{kC_0 D_A} \tag{4}$$

is selected [3, 4, 27]. The parameter $C_0 = A(x, 0) + B(x, 0)$ is the sum of the initial concentrations of species A and B. Discrete variables of space, $i = x/\Delta x$, and time, $s = t/\Delta t$, where Δx is the cell length and Δt is the time step, are introduced in order to numerically solve Eqs. (2) and (3) in a wide range of diffusion coefficients D_B. We consider a system of $\ell = 2000$ spatial cells. The initial condition is a step function located in the cell $i_0 = \ell/2$

$$A(i, 0) = C_0 H(i_0 - i), \tag{5}$$

$$B(i, 0) = C_0 H(i - i_0), \tag{6}$$

3

where $H(i)$ is the Heaviside function. In order to simulate a moving frame and to counterbalance the autocatalytic production of species A in a finite system, the following procedure is applied. At the time steps s such that $\sum_{i=1}^{\ell} A(i, s) > \sum_{i=1}^{\ell} A(i, 0)$, the first cell is suppressed and a last cell with $A(\ell, s) = 0$ and $B(\ell, s) = C_0$ is created. Hence, the inflection point of the front profile remains close to the initial step of the Heaviside function.

In small systems with typically hundreds of particles per spatial cell, the deterministic description may fail and a stochastic approach is required. We consider the chemical master equation associated with Eq. (1) [32, 33]. The master equation is divided into two parts

$$\frac{\partial P(\phi)}{\partial t} = \left.\frac{\partial P(\phi)}{\partial t}\right|_{\text{reaction}} + \left.\frac{\partial P(\phi)}{\partial t}\right|_{\text{diffusion}} \tag{7}$$

where the first part corresponds to the reactive terms

$$\left.\frac{\partial P(\phi)}{\partial t}\right|_{\text{reac}} = \sum_i \frac{k}{\Omega N_0}\Big[(N_A(i) - 1)(N_B(i) + 1)P(\{N_A(i) - 1, N_B(i) + 1\})$$
$$- N_A(i)N_B(i)P(\phi)\Big] \tag{8}$$

and the second part corresponds to the diffusion terms

$$\left.\frac{\partial P(\phi)}{\partial t}\right|_{\text{diff}} = \sum_i \Big[\frac{D_A}{\Delta x^2}(N_A(i) + 1)\Big[P(\{N_A(i-1) - 1, N_A(i) + 1\})$$
$$+ P(\{N_A(i) + 1, N_A(i+1) - 1\})\Big]$$
$$+ \frac{D_B}{\Delta x^2}(N_B(i) + 1)\Big[P(\{N_B(i-1) - 1, N_B(i) + 1\})$$
$$+ P(\{N_B(i) + 1, N_B(i+1) - 1\})\Big]$$
$$- \frac{2}{\Delta x^2}\Big(D_A N_A(i) + D_B N_B(i)\Big)P(\phi)\Big] \tag{9}$$

where $\phi = \{N_A(i), N_B(i)\}$ denotes the default state, Ω, the typical size of the system, $N_0 = \Omega C_0$, the initial total number of particles in a cell, and $N_A(i) = \Omega A(i)$ and $N_B(i) = \Omega B(i)$ are the numbers of particles A and B in cell i. We consider parameter values leading to the macroscopic values used in the deterministic approach. The initial condition is given by $(N_A(i) = N_0, N_B(i) = 0)$ for $1 \leq i < \ell/2$ and $(N_A(i) = 0, N_B(i) = N_0)$ for $\ell/2 \leq i \leq \ell$ with $N_0 = 100$, $\Omega = 10$ ($C_0 = 10$).
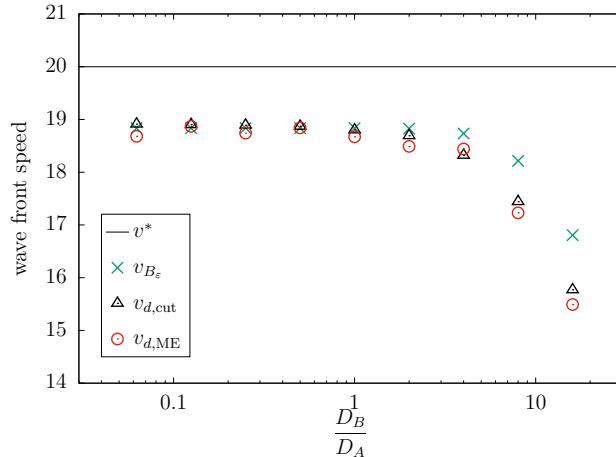
Figure 1: Dilute system. Wave front speeds $v_{d,\mathrm{ME}}$, $v_{d,\mathrm{cut}}$, v_{B_ε}, and $v_d = v^*$ versus ratio of diffusion coefficients D_B/D_A in the dilute case. The values of $v_{d,\mathrm{ME}}$ (red circles) are deduced from the direct simulation of the master equation (Eqs. (7-9)) for $k = 10$, $\Omega = 10$, $N_0 = 100$, $D_A = 1$, $\ell = 2000$, and $\Delta x = 0.008$. The values of $v_{d,\mathrm{cut}}$ (black open triangles) are deduced from the numerical integration of the deterministic equations (Eqs. (14) and (15)) in the presence of a cutoff $\varepsilon = 10^{-4}$ for $k = 10$, $C_0 = 10$, $D_A = 1$, $\ell = 2000$, $\Delta x = 0.008$, and $\Delta t = 6.4 \times 10^{-6}$. The values of v_{B_ε} (green crosses) are deduced from Eq. (16) in which the value B_ε has been deduced from the numerical integration of Eqs. (14) and (15). The horizontal line gives the minimum velocity $v_d = v^*$ (Eq. (4)) of an FKPP front in the absence of a cutoff.

The kinetic Monte Carlo algorithm developed by Gillespie is used to directly simulate the reaction and diffusion processes and numerically solve the master equation [34]. The procedure used in the deterministic approach to evaluate the front speed is straightforwardly extended to the fluctuating system.

2.1   Front speed

For sufficiently small spatial lengths Δx and time steps Δt, the numerical solution of the deterministic equations given in Eqs. (2) and (3) leads to the same propagation speed v_d, where the index d stands for dilute, in the entire range of D_B/D_A values [12]. The number of cells created during 10^7 time steps once a stationary propagation is reached is used to evaluate the front speed. For the chosen parameter values, we find a propagation speed obeying $v_d = v^* = 20$ with an accuracy of 0.4%: No appreciable deviation from the unperturbed deterministic prediction given in Eq. (4) is observed. In particular, the front speed v_d does not depend on the diffusion coefficient D_B. The front speed deduced from the direct simulation of Eqs. (7-9) is denoted $v_{d,\mathrm{ME}}$ where the index d stands for dilute

5

and the index ME for master equation. As shown in Fig. 1, the velocity $v_{d,\mathrm{ME}}$ is smaller than the deterministic prediction v^* given in Eq. (4).

As long as D_B remains smaller than or equal to D_A, the velocity $v_{d,\mathrm{ME}}$ is constant. The main result of the master equation approach is that the front speed drops as D_B increases above D_A. Typically, for $D_B/D_A = 16$, the velocity $v_{d,\mathrm{ME}}$ is reduced by 22% with respect to $v_d = v^*$. Due to computational costs, larger D_B/D_A values were not investigated.

In the case of identical diffusion coefficients for the two species, the decrease of the front speed observed in a stochastic description is interpreted in the framework of the cutoff approach introduced by Brunet and Derrida [27]. For $D_A = D_B$, the dynamics of the system is described by a single equation. When a cutoff ε is introduced in the reactive term according to

$$\partial_t A = \partial_x^2 A + kA(C_0 - A)H(A - \varepsilon), \tag{10}$$

the velocity is given by

$$v_\varepsilon = v^* \left(1 - \frac{\pi^2}{2(\ln \varepsilon)^2} \right) \tag{11}$$

In a particle description, the cutoff is interpreted as the inverse of the total number of particles in the reactive interface [28]:

$$\varepsilon = \frac{\Delta x}{N_0 W^*} \tag{12}$$

where the width of the interface is roughly evaluated at [4, 12]

$$W^* = 8\sqrt{\frac{D_A}{kC_0}} \tag{13}$$

For the chosen parameter values, the cutoff equals $\varepsilon = 10^{-4}$ leading to the corrected speed $v_\varepsilon = 18.84$. According to Fig. 1, the velocity $v_{d,\mathrm{ME}}$ deduced from the master equation for $D_A = D_B$ agree with the velocity v_ε deduced from the cutoff approach. The results are unchanged for $D_B < D_A$ and Eq. (11) correctly predicts the velocity in a fluctuating system. For $D_B > D_A$, Eq. (11) is not valid. Nevertheless, the relevance of the cutoff approach can be checked by numerically integrating the two following equations

$$\partial_t A \ = D_A \partial_x^2 A + kABH(A - \varepsilon) \tag{14}$$

$$\partial_t B \ = D_B \partial_x^2 B - kABH(A - \varepsilon) \tag{15}$$

6

The values of the front speed $v_{d,\text{cut}}$ deduced from the numerical integration of Eqs. (14) and (15) are given in Fig. 1 and satisfactorily agree with the results $v_{d,\text{ME}}$ of the master equation, including for large D_B/D_A values.

According to Fig. 2a, the A profile is steeper than the B profile for $D_B > D_A$. The mean number of B particles in the leading edge smoothly converges to N_0. In average, the rightmost A particle sees a number of B particles smaller than N_0. The significant decrease of the front velocity $v_{d,\text{cut}}$ for $D_B > D_A$ is qualitatively interpreted by the apparent number N_ε of B particles seen by the rightmost A particle in the leading edge. The linear analysis of Eqs. (14) and (15) according to the cutoff approach [27] leads to Eq. (11) which does not account for the behavior at large D_B. A nonlinear analysis would be necessary. Using the perturbative approach that we developed in the case of the deterministic description [4, 12], applying the Hamilton-Jacobi technique [35, 36], or deducing the variance $\langle AB \rangle$ from a Langevin approach [37], we unsuccessfully tried to find an analytical estimation of the front speed. Instead, we suggest the following empirical expression of the velocity of an FKPP front for two species with different diffusion coefficients

$$v_{B_\varepsilon} = 2\sqrt{kB_\varepsilon D_A}\left(1 - \frac{\pi^2}{2(\ln\varepsilon)^2}\right) \tag{16}$$

where B_ε denotes the concentration of B species at the abscissa x_ε at which the scaled concentration $A(x_\varepsilon)/C_0$ is equal to the cutoff ε (see Fig. 2b). The variation of B_ε versus D_B/D_A is numerically evaluated using Eqs. (14) and (15). The result is given in Fig. 3.

As shown in Fig. 1, the variation of the front speed v_{B_ε} with D_B/D_A deduced from Eq. (16) slightly underestimates the results $v_{d,\text{cut}}$ deduced from the numerical integration of the deterministic equations (Eqs. (14) and (15)) with a cutoff.

2.2 Profile properties

We focus on two steady properties of the wave front, the shift between the profiles of species A and B and the width of species A profile [12].

For a wave front propagating at speed v and using the coordinate $z = x - vt$ in the moving frame, the shift between the profiles of the two species is defined as the difference $A(z = 0) - B(z = 0)$ of concentrations between species A and B at the origin $z = 0$
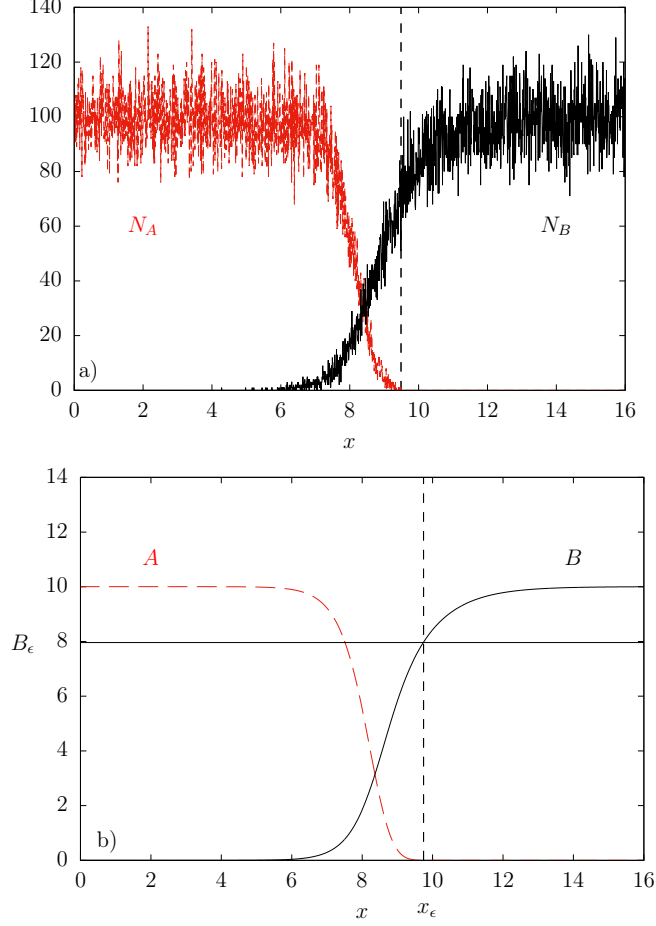
Figure 2: Dilute system. (a) Numbers N_A of particles A (red dashed line) and N_B of particles B (black solid line) versus spatial coordinate x deduced from direct simulation of the master equation (Eqs. (7-9)) using Gillespie method. The snapshot is given at time $t = 9$ for $k = 10$, $\Omega = 10$, $N_0 = 100$, $D_A = 1$, $D_B = 16$, $\ell = 2000$, and $\Delta x = 0.008$. The vertical dashed line indicates the rightmost cell occupied by A particles. (b) Concentrations A of species A (red dashed line) and B of species B (black solid line) versus spatial coordinate x deduced from numerical integration of the deterministic equations (Eqs. (14) and (15)) in the presence of a cutoff $\varepsilon = 10^{-4}$. The snapshot is given at time $t = 640$ for the same other parameters as in the master equation approach. The vertical dashed line indicates the abscissa x_ε for which the scaled A concentration $A(x_\varepsilon)/C_0$ reaches the cutoff value. The horizontal line indicates the value B_ε of B concentration at the abscissa x_ε.
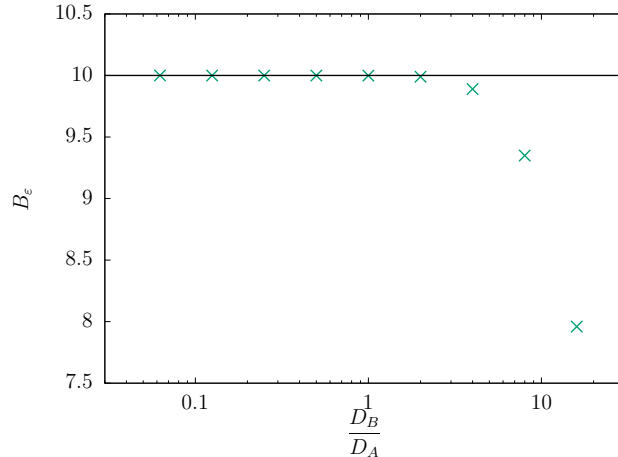
Figure 3: Dilute system. The green crosses give the value B_ε deduced from the numerical integration of the deterministic equations (Eqs. (14) and (15)) with a cutoff $\varepsilon = 10^{-4}$ versus the ratio of the diffusion coefficients D_B/D_A. The horizontal line indicates the concentration C_0. The parameters are given in the caption of Fig. 1.

chosen such that $A(z=0) = C_0/2$. The shift is denoted by h_d, where the index d stands for dilute, when the concentrations are solutions of the deterministic equations without cutoff given in Eqs. (2) and (3). As shown in Fig. 4, the shift h_d significantly varies with the ratio D_B/D_A, in particular when D_B is larger than D_A [12]. The shift vanishes for $D_A = D_B$, is positive for $D_B < D_A$ and negative for $D_B > D_A$.

The direct simulation of the master equation leads to highly fluctuating profiles. We use the following strategy to compute the shift $h_{d,\mathrm{ME}}$. First, starting from the leftmost cell, we scan to the right to determine the label i_l of the first cell in which the number of A particles drops under $N_0/2$ and store $N_B(i_l, s)$ for a large discrete time s at which the profile has reached a steady shape. Then, starting from the rightmost cell labeled ℓ, we follow a similar procedure and determine the label i_r of the first cell in which the number of A particles overcomes $N_0/2$ and store $N_B(i_r, s)$ for the same discrete time s. The instantaneous value of the shift deduced from the master equation at discrete time s is then given by $(N_0 - N_B(i_l, s) - N_B(i_r, s))/2\Omega$. The values of the shift $h_{d,\mathrm{ME}}$ used to draw Fig. 4 are obtained after a time average between the times $t = 1$ and $t = 10$ in arbitrary units, i.e. between $s = 1.5 \times 10^5$ and $s = 1.5 \times 10^6$ in number of time steps.

The shift $h_{d,\mathrm{ME}}$ between the profiles of A and B is sensitive to the fluctuations of the number of particles described by the master equation. Introducing an appropriate cutoff satisfying Eq. (12) in the reactive term of the deterministic equations given in Eqs. (14)
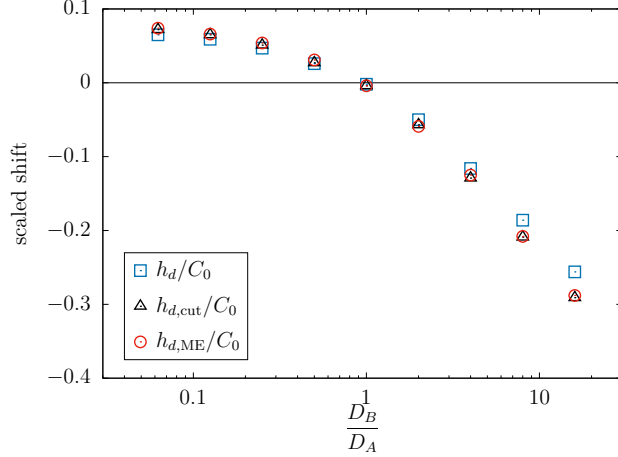
Figure 4: Dilute system. Scaled shifts $h_{d,\mathrm{ME}}/C_0$, $h_{d,\mathrm{cut}}/C_0$, and h_d/C_0 between the profiles of species A and B versus ratio of diffusion coefficients D_B/D_A. The values of $h_{d,\mathrm{ME}}/C_0$ (red circles) are deduced from the master equation (Eqs. (7-9)). The values of $h_{d,\mathrm{cut}}/C_0$ (black open triangles) are deduced from the deterministic equations (Eqs. (14 and 15)) with a cutoff $\varepsilon = 10^{-4}$. The values of h_d/C_0 (blue open squares) are deduced from the deterministic equations (Eqs. (2) and (3)) without cutoff. The line gives the results for $D_A = D_B$. The parameters are given in the caption of Fig. 1.

and (15) leads to values of the shift $h_{d,\mathrm{cut}}$ in very good agreement with the results $h_{d,\mathrm{ME}}$ of the master equation.

Considering the deterministic equations, we deduce the width of A profile from the steepness $A'(0)$ in the moving frame at the origin $z = 0$ and find

$$W_d = C_0/|A'(0)| \tag{17}$$

where A is solution of Eqs. (2) and (3) without cutoff. The same definition is applied to Eqs. (14) and (15) to obtain the width $W_{d,\mathrm{cut}}$ in the presence of a cutoff. The definition has to be adapted to take into account the fluctuations of the profile deduced from the master equation. Using the cell labels i_l and i_r determined for the shift between the fluctuating A and B profiles solutions of Eqs. (7-9), we define the mean cell label i_m as the nearest integer to the average $(i_l + i_r)/2$. We use Eq. (17) with $|A'(0)| \simeq (N_A(i_m - 40) - N_A(i_m + 40))/(81\Delta x \Omega)$ to compute the instantaneous width. As in the case of the shift $h_{d,\mathrm{ME}}$ between the fluctuating profiles of A and B, the values $W_{d,\mathrm{ME}}$ of the width used to draw Fig. 5 are obtained after a time average between the times $t = 1$ and $t = 10$.

As shown in Fig. 5, the width W_d deduced from the deterministic equations without cutoff is smaller (resp. larger) for $D_B < D_A$ (resp. $D_B > D_A$) than the width evaluated
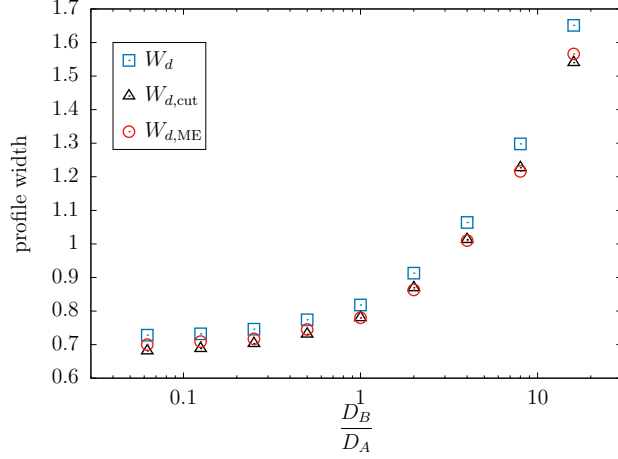
10

Figure 5: Dilute system. Profile widths deduced from different approaches versus ratio of diffusion coefficients D_B/D_A. The values of $W_{d,\mathrm{ME}}$ (red circles) are deduced from the master equation (Eqs. (7-9)). The values of $W_{d,\mathrm{cut}}$ (black open triangles) are deduced from the numerical integration of the deterministic equations (Eqs. (14) and (15)) with a cutoff $\varepsilon = 10^{-4}$. The values of W_d (blue open squares) are deduced from the numerical integration of the deterministic equations (Eqs. (2) and (3)) without cutoff. The parameters are given in the caption of Fig. 1.

at W^* in the case of identical diffusion coefficients $D_B = D_A$ [12]. The width $W_{d,\mathrm{ME}}$ deduced from the master equation (Eqs. (7-9)) and the width $W_{d,\mathrm{cut}}$ deduced from the deterministic equations (Eqs. (14) and (15)) with a cutoff obeying Eq. (12) agree and are both smaller than the width W_d of the wave front, solution of the deterministic equations without cutoff.

According to the good agreement between the results of the master equation and the deterministic equations with a cutoff, it is more relevant to describe the effect of the fluctuations on the wave front as the effect of the discretization of the variables than a pure noise effect.

Figure 6 summarizes the effect of the fluctuations on the three quantities q for $q = v, h, W$ in the whole range of considered values of the ratio D_B/D_A for the dilute system. The relative differences $(q_{d,\mathrm{ME}} - q_d)/q_d$ between the results deduced from the master equation and the deterministic equations without cutoff are given in Fig. 6 for the velocity, the shift, and the width. In the whole range of D_B/D_A, the discrete nature of the number of particles in the master equation induces a small decrease of 5% of the profile width with respect to the deterministic description without cutoff. A significant increase of 14% of the shift between the A and B profiles is observed in the presence of fluctuations in the
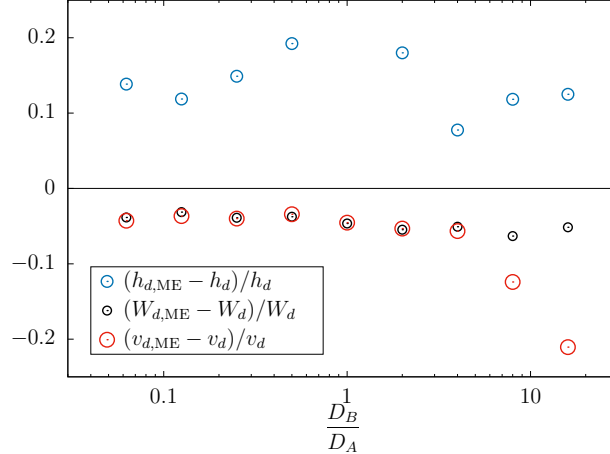
11

Figure 6: Dilute system. Relative differences between the front properties deduced from the master equation (Eqs. (7-9)) and the analogous properties deduced from the deterministic equations without cutoff (Eqs. (2 and (3)) versus D_B/D_A. The large red circles give the relative difference $(v_{d,\mathrm{ME}} - v_d)/v_d$ for the front speed, the blue circles of intermediate size give the relative difference $(h_{d,\mathrm{ME}} - h_d)/h_d$ for the shift between A and B profiles, and the small black circles give the relative difference $(W_{d,\mathrm{ME}} - W_d)/W_d$ for the width of A profile. The parameters are given in the caption of Fig. 1.

entire interval of ratios of diffusion coefficients. As for the width, the relative difference of velocity $(v_{d,\mathrm{ME}} - v_d)/v_d$, with $v_d = v^*$, is negative and takes the same value of -5% for $D_B/D_A \leq 1$. However, the relative difference of velocity is not constant for $D_B/D_A > 1$ and reaches -22% for $D_B/D_A = 16$. Hence, a significant speed decrease is observed whereas the shift and the width, far behind the leading edge of the front, are not affected by large diffusion coefficients of species B with respect to the diffusion coefficient of species A.

3 Concentrated system

In a dilute system, the solvent S is in great excess with respect to the reactive species A and B. The concentration of the solvent is then supposed to remain homogeneous regardless of the variation of concentrations A and B. In a concentrated solution, the variation of the concentration of the solvent cannot be ignored. In the linear domain of irreversible thermodynamics, the diffusion fluxes are linear combinations of the concentration gradients of the different species. The flux j_X of species X=A, B, S depends on the concentration gradients and the diffusion coefficients of all species A, B, and S [38, 39]. Using the conservation relations $C_{tot} = A + B + S$, where C_{tot} is a constant, we eliminate

12

the explicit dependence of the fluxes on the concentration S of the solvent and find

$$j_A = -\left(1 - \frac{A}{C_{tot}}\right)D_A\partial_x A + \frac{A}{C_{tot}}D_B\partial_x B \tag{18}$$

$$j_B = \frac{B}{C_{tot}}D_A\partial_x A - \left(1 - \frac{B}{C_{tot}}\right)D_B\partial_x B \tag{19}$$

According to the expression of the diffusion fluxes in a concentrated system, the reaction-diffusion equations associated with the chemical mechanism given in Eq. (1) read [39]

$$\partial_t A = D_A\partial_x\left[\left(1 - \frac{A}{C_{tot}}\right)\partial_x A\right] - D_B\partial_x\left(\frac{A}{C_{tot}}\partial_x B\right) + kAB \tag{20}$$

$$\partial_t B = D_B\partial_x\left[\left(1 - \frac{B}{C_{tot}}\right)\partial_x B\right] - D_A\partial_x\left(\frac{B}{C_{tot}}\partial_x A\right) - kAB \tag{21}$$

The discrete expression of the flux at the interface between cells i and $i+1$ is related to the difference of the transition rates in the master equation according to

$$j_X(i + 1/2) = -\frac{1}{\Delta x}\left(T^-_{N_X(i+1)} - T^+_{N_X(i)}\right) \tag{22}$$

where $X = A, B$, the transition rate $T^-_{N_X(i+1)}$ is associated with the jump of a particle X to the left from cell $i+1$ to cell i, and $T^+_{N_X(i)}$ is associated with the jump of a particle X to the right from cell i to cell $i+1$. Using Eqs. (18) and (19) and replacing $\partial_x X$ by $(N_X(i+1) - N_X(i))/\Omega\Delta x$ for $X = A, B$, we assign well-chosen terms of the flux $j_X(i+1/2)$ to the transition rates to the left and to the right

$$T^\pm_{N_A(i)} = \frac{D_A}{\Delta x^2}N_A(i) - \frac{N_A(i \pm 1/2)}{\Omega C_{tot}\Delta x^2}\left[D_A N_A(i) - D_B N_B(i \pm 1)\right] \tag{23}$$

$$T^\pm_{N_B(i)} = \frac{D_B}{\Delta x^2}N_B(i) - \frac{N_B(i \pm 1/2)}{\Omega C_{tot}\Delta x^2}\left[D_B N_B(i) - D_A N_A(i \pm 1)\right] \tag{24}$$

to ensure that they are positive or equal to zero for any number of particles. A standard arithmetic mean for the number $N_X(i \pm 1/2)$ of particles $X = A, B$ in the virtual cell $i \pm 1/2$ cannot be used since it may lead to a non-zero transition rate when the departure cell is empty. Instead, we choose the harmonic mean between the number of particles in cells i and $i \pm 1$:

$$N_X(i \pm 1/2) = \frac{N_X(i)N_X(i \pm 1)}{N_X(i) + N_X(i \pm 1)} \tag{25}$$

which ensures that no jump of X from cell i to cell $i \pm 1$ occurs when the number of particles N_X vanishes in cell i. We checked different definitions of the mean obeying

13

the latter condition and found that the results are not significantly affected when choosing for $N_X(i \pm 1/2)$ a modified arithmetic mean which vanishes if $N_X(i) = 0$ and equals $(N_X(i) + N_X(i \pm 1))/2$ otherwise, or a geometric mean $\sqrt{N_X(i)N_X(i \pm 1)}$.

It is worth noting that, contrary to the dilute case for which the transition rate associated with the diffusion of particles X only depends on the number of particles X in the departure cell, the transition rate in the concentrated case also depends on the number of particles A and B in the arrival cell. In the case of a concentrated system, the diffusion term reads

$$
\begin{aligned}
\frac{\partial P(\phi)}{\partial t}\bigg|_{\text{diff}} = \sum_i \bigg[& T^-_{N_A(i)+1} P(\{N_A(i-1)-1, N_A(i)+1\}) \\
& + T^+_{N_A(i)+1} P(\{N_A(i)+1, N_A(i+1)-1\}) \\
& + T^-_{N_B(i)+1} P(\{N_B(i-1)-1, N_B(i)+1\}) \\
& + T^+_{N_B(i)+1} P(\{N_B(i)+1, N_B(i+1)-1\}) \\
& - \left(T^-_{N_A(i)} + T^+_{N_A(i)} + T^-_{N_B(i)} + T^+_{N_B(i)} \right) P(\phi) \bigg]
\end{aligned}
\tag{26}
$$

The reaction term $\dfrac{\partial P(\phi)}{\partial t}\bigg|_{\text{reac}}$ of the master equation given in Eq. (8) for the dilute system is unchanged in the case of a concentrated system. The kinetic Monte Carlo algorithm and the initial and boundary conditions used for the dilute system are straightforwardly extended to the concentrated system.

The front speeds $v_{c,\text{ME}}$ and $v_{d,\text{ME}}$ deduced from the master equation in concentrated and dilute cases, respectively, are compared in Fig. 7. The correction to the wave front speed induced by an increase of the ratio of diffusion coefficients D_B/D_A is smaller for a concentrated system than for a dilute system. Indeed, in the concentrated case, the diffusion of a species depends on the diffusion coefficients of both species. Hence, increasing D_B at constant D_A has a smaller impact on the velocity since the contribution depending on D_B is partly compensated by the unchanged terms depending on D_A.

The effect of the departure from the dilution limit on the wave front speed $v_{c,\text{ME}}$ deduced from the master equation given in Eqs. (7), (8), and (26) is shown in Fig. 8. The dilution limit $v_{d,\text{ME}}(D_B/D_A = 8) = 17.20$ is recovered for $C_0/C_{tot} \to 0$. As C_0/C_{tot}
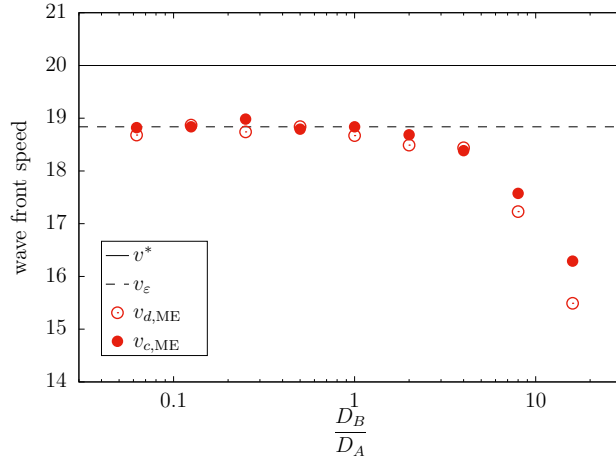
14

Figure 7: Concentrated system. Wave front speed $v_{c,\mathrm{ME}}$ deduced from the master equation (Eqs. (7), (8), and (26)) in a concentrated system (red solid disks) for $C_{tot} = 50$ and speed $v_{d,\mathrm{ME}}$ deduced from the direct simulation of the master equation (Eqs. (7-9)) associated with the dilute system (red circles) versus ratio of diffusion coefficients D_B/D_A. The horizontal solid line gives the minimum velocity v^* (Eq. (4)) of an FKPP front in the absence of a cutoff. The horizontal dashed line gives the velocity $v_\varepsilon = 18.84$ given in Eq. (11) for a cutoff $\varepsilon = 10^{-4}$ and $D_A = D_B$. The parameters are given in the caption of Fig. 1.
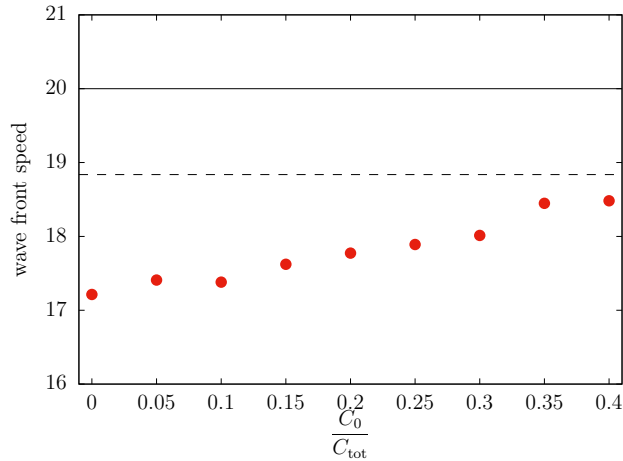

Figure 8: Concentrated system. Wave front speeds versus the deviation from the dilution limit C_0/C_{tot}. The values of $v_{c,\mathrm{ME}}$ (red disks) are deduced from the direct simulation of the master equation (Eqs. (7), (8), and (26)) for $k = 10$, $\Omega = 10$, $N_0 = 100$, $D_A = 1$, $D_B = 8$, $\ell = 2000$, and $\Delta x = 0.008$ ($C_0 = N_0/\Omega$). The horizontal solid line gives the minimum velocity $v^* = 20$ (Eq. (4)) of an FKPP front, solution of the deterministic equations (Eqs. (2) and (3)) without cutoff. The horizontal dashed line gives the velocity $v_\varepsilon = 18.84$ given in Eq. (11) for a cutoff $\varepsilon = 10^{-4}$ and $D_A = D_B$.
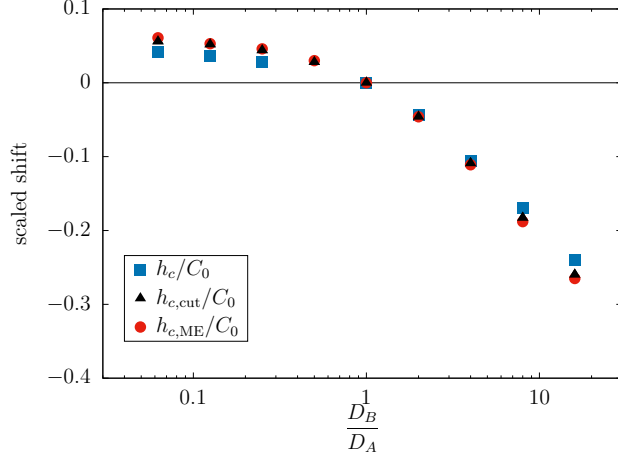
Figure 9: Concentrated system. Scaled shifts $h_{c,\mathrm{ME}}/C_0$, $h_{c,\mathrm{cut}}/C_0$, and h_c/C_0 between the profiles of species A and B versus ratio of diffusion coefficients D_B/D_A. The values of $h_{c,\mathrm{ME}}/C_0$ (red disks) are deduced from the master equation (Eqs. (7), (8), and (26)). The values of $h_{c,\mathrm{cut}}/C_0$ (black solid triangles) are deduced from the deterministic equations (Eqs. (20) and (21)) with a reactive term multiplied by the cutoff $H(A-\varepsilon)$ for $\varepsilon = 10^{-4}$. The values of h_c/C_0 (blue solid squares) are deduced from the deterministic equations (Eqs. (20) and (21)) without cutoff. The other parameters are given in the caption of Fig. 7. The line gives the results for $D_A = D_B$.

increases, the solution is more concentrated and the cross-diffusion terms become more important, so that the system is less sensitive to the difference between the diffusion coefficients D_A and D_B: The wave front speed $v_{c,\mathrm{ME}}$ increases and tends to the value $v_\varepsilon = 18.84$ predicted by Eq. (11) for the cutoff $\varepsilon = 10^{-4}$ and $D_A = D_B$.

The variation of the shifts $h_{c,\mathrm{ME}}$, $h_{c,\mathrm{cut}}$, and h_c between the two profiles with respect to the ratio of the diffusion coefficients D_B/D_A is shown in Fig. 9 in a concentrated system for the three approaches, the master equation and the deterministic descriptions with and without cutoff. As revealed when comparing the results given in Figs. 4 and 9, the effect of the departure from the dilution limit on the shift is too small for us to evaluate the difference $(h_{c,\mathrm{ME}} - h_{d,\mathrm{ME}})/h_{d,\mathrm{ME}}$ with a sufficient precision for the fluctuating results deduced from the master equations.

The effects of the departure from the dilution limit on the widths $W_{c,\mathrm{ME}}$, $W_{c,\mathrm{cut}}$, and W_c of the profile are given in Fig. 10 for the three approaches. The agreement between the results $W_{c,\mathrm{ME}}$ and $W_{c,\mathrm{cut}}$ deduced from the master equation (Eqs. (7), (8), and (26)) and the deterministic equations (Eqs. (14 and 15)) with a cutoff, respectively, is satisfying
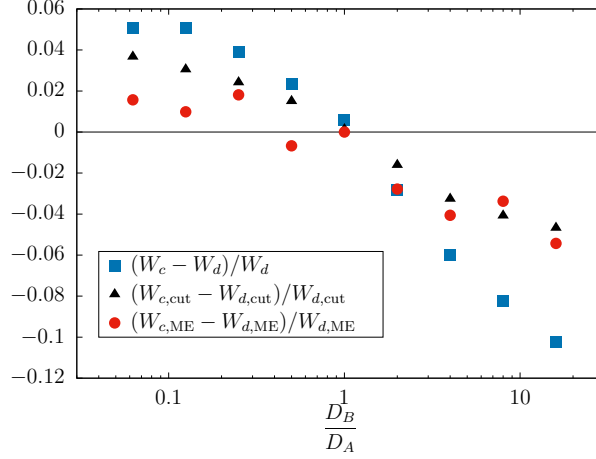
16

Figure 10: Relative differences $(W_{c,\mathrm{ME}} - W_{d,\mathrm{ME}})/W_{d,\mathrm{ME}}$, $(W_{c,\mathrm{cut}} - W_{d,\mathrm{cut}})/W_{d,\mathrm{cut}}$, and $(W_c - W_d)/W_d$ between the widths in a concentrated system and a dilute system for different approaches versus D_B/D_A. The values of $W_{c,\mathrm{ME}}$ and $W_{d,\mathrm{ME}}$ (red disks) are deduced from the master equation (Eqs. (7), (8), and (26) and Eqs. (7-9), respectively). The values of $W_{c,\mathrm{cut}}$ and $W_{d,\mathrm{cut}}$ (black solid triangles) are deduced from the deterministic equations (Eqs. (20) and (21) and Eqs. (14) and (15), respectively) with a reactive term multiplied by the cutoff $H(A - \varepsilon)$ for $\varepsilon = 10^{-4}$. The values of W_c and W_d (blue solid squares) are deduced from the deterministic equations (Eqs. (20) and (21) and Eqs. (2) and (3), respectively) without cutoff.

considering the high level of noise on the evaluation of the width $W_{c,\mathrm{ME}}$. According to Fig. 5, the width in a dilute system is smaller than the width obtained for identical diffusion coefficients if $D_B < D_A$ and larger if $D_B > D_A$. The results displayed in Fig. 10 prove that, for each description method, the width in a concentrated system is larger than the width in a dilute system if $D_B < D_A$ and smaller if $D_B > D_A$. Hence, in the entire range of ratios of diffusion coefficients and for deterministic as well as stochastic methods, the width in a concentrated system is closer to the width obtained for identical diffusion coefficients. As for the front speed, the departure from the dilution limit reduces the effects induced by the difference between the diffusion coefficients.

4 Conclusion

We have performed kinetic Monte Carlo simulations of the master equation associated with a chemical system involving two species A and B. The two species have two different diffusion coefficients, D_A and D_B, and are engaged in the autocatalytic reaction $\mathrm{A} + \mathrm{B} \rightarrow 2\mathrm{A}$. The effects of fluctuations on the FKPP wave front have been studied in the cases of

a dilute solution and a concentrated solution in which cross-diffusion cannot be neglected.

In the case of a dilute system, the linearization of the deterministic equations with a cutoff in the leading edge of the front leads to a speed shift independent of the diffusion coefficient D_B of the consumed species. The speed shift obtained for two different diffusion coefficients is the same as in the case $D_A = D_B$. The main result deduced from the master equation is that the front speed sensitively depends on the diffusion coefficient D_B. For D_B larger than D_A, the front speed decreases as D_B increases and is significantly smaller than the prediction of the linear cutoff theory. The speed decrease obtained for large values of D_B/D_A is related to the number N_{B_ε} of B particles at the position of the most advanced A particle in the leading edge of the front. When species B diffuses faster that species A, N_{B_ε} is significantly smaller than the steady-state value N_0.

We carefully derived the nontrivial expression of the master equation in a concentrated system with cross-diffusion. The transition rates are deduced from the diffusion fluxes in the linear domain of irreversible thermodynamics. The transition rates associated with diffusion depend on the number of particles not only in the departure cell but also in the arrival cell. Qualitatively, the conclusions drawn for a dilute solution and $D_A \neq D_B$ remain valid, but the front properties deduced from the master equation with cross-diffusion depart less from those obtained for $D_A = D_B$. The dependence of the front properties on D_B/D_A in a concentrated system are softened with respect to the dilute case. Cross-diffusion mitigates the impact of the difference between the diffusion coefficients.

5 Acknowledgments

References

[1] R. A. Fisher, Annals of Eugenics **7**, 355 (1937).

[2] A. N. Kolmogorov, I.G. Petrovsky, and N.S. Piskunov, Bulletin of Moscow State University Series A: Mathematics and Mechanics **1**, 1-25 (1937).

[3] W. van Saarloos, Phys. Rep. **386** 29-222 (2003).

[4] J. D. Murray, *Mathematical Biology* (Springer, Berlin, 1989).

[5] V. Mendez, D. Campos, and F. Bartumeus, *Stochastic Foundations in Movement Ecology: Anomalous diffusion, invasion fronts and random searches* (Springer, Berlin, 2014).

[6] E. Bouin, V. Calvez, N. Meunier, S. Mirrahimi, B. Perthame, G. Raoul, R. Voituriez, C. R. Acad. Sci. Paris, Ser. I **350**, 761 (2012).

[7] J. Fort, N. Isern, A. Jerardino, and B. Rondelli, p. 189-197, in Simulating Prehistoric and Ancient Worlds, Eds. J. A. Baracelo and F. Del Castillo, Springer, Cham (2016).

[8] R. Mancinelli, D. Vergni, A. Vulpiani, Physica D **185**, 175 (2003).

[9] D. Froemberg, H. Schmidt-Martens, I. M. Sokolov, and F. Sagues, Phys. Rev. E **78**, 011128 (2008).

[10] X. Cabré and J.-M. Roquejoffre, C. R. Acad. Sci. Paris, Ser. I **347**, 1361 (2009).

[11] F. El Adnani and H. Talibi Alaoui, Topol. Methods Nonlinear Anal. **35**, 43 (2010).

[12] G. Morgado, B. Nowakowski, and A. Lemarchand, Phys. Rev. E **99**, 022205 (2019).

[13] V. K. Vanag and I. R. Epstein, Phys. Chem. Chem. Phys. **11**, 897-912 (2009).

[14] D. G. Leaist, Phys. Chem. Chem. Phys. **4**, 4732–4739 (2002).

[15] V. K. Vanag, F. Rossi, A. Cherkashin, and I. R. Epstein, J. Phys. Chem. B **112**, 9058–9070 (2008).

[16] F. Rossi, V. K. Vanag, and I. R. Epstein, Chem. A Eur. J. **17**, 2138–2145 (2011).

[17] M. A. Budroni, L. Lemaigre, A. De Wit and F. Rossi, Phys. Chem. Chem. Phys. **17**, 1593 (2015).

[18] M. A. Budroni, J. Carballido-Landeira, A. Intiso, A. De Wit, and F. Rossi, Chaos **25**, 064502 (2015).

[19] L. Desvillettes, Th. Lepoutre, and A. Moussa, SIAM J. Math. Anal. **46**, 820 (2014).

[20] L. Desvillettes and A. Trescases, J. Math. Anal. Appl. **430**, 32 (2015).

[21] L. Desvillettes, T. Lepoutre, A. Moussa, and A. Trescases, Commun. Part. Diff. Eq. **40**, 1705 (2015).

[22] *Advances in Reaction-Cross-Diffusion Systems*, A. Jüngel, L. Chen, and L. Desvillettes, Eds, Nonlinear anal. **159**, 1-492 (2017).

[23] E. Daus, L. Desvillettes, H. Dietert, J. Differ. Equ. **266**, 3861 (2019).

[24] A. Moussa, B. Perthame, and D. Salort, J. Nonlinear Sci. **29**, 139 (2019).

[25] H. P. Breuer, W. Huber, and F. Petruccione, Physica D **73**, 259 (1994).

[26] A. Lemarchand, A. Lesne, and M. Mareschal, Phys. Rev. E **51**, 4457 (1995).

[27] E. Brunet and B. Derrida, Phys. Rev. E **56**, 2597 (1997).

[28] J. S. Hansen, B. Nowakowski and A. Lemarchand, J. Chem. Phys. **124**, 034503 (2006).

[29] D. Panja, Phys. Rep. **393**, 87-174 (2004).

[30] J. G. Conlon and C. R. Doering, J. Stat. Phys. **120**, 421 (2005).

[31] J. Mai, I. M. Sokolov, V. N. Kuzovkov, and A. Blumen, Phys. Rev. E **56**, 4130 (1997).

[32] G. Nicolis and I. Prigogine, *Self-Organization in Nonequilibrium Systems* (Wiley, New York, 1977).

[33] C.W. Gardiner, *Handbook of Stochastic Methods for Physics, Chemistry and the Natural Sciences* (Springer, Berlin, 1985).

[34] D. T. Gillespie, J. Chem. Phys. **81**, 2340 (1977).

[35] Wave front for a reaction-diffusion system and relativistic Hamilton-Jacobi dynamics S. Fedotov, Phys. Rev. E **59**, 5040 (1999).

[36] S. Mirrahimi, G. Barles, B. Perthame, and P.E. Souganidis, SIAM J. Math. Anal. **44**, 4297 (2012).

[37] C. Bianca and A. Lemarchand, Physica A **438**, 1 (2015).

[38] S. R. de Groot and P. Mazur, *Non-Equilibrium Thermodynamics* (North-Holland, Amsterdam, 1962).

[39] L. Signon, B. Nowakowski, and A. Lemarchand, Phys. Rev. E **93**, 042402 (2016).